

Coupled-mode theory of diffraction-induced transverse effects in nonlinear optical resonators

R. Reinisch and G. Vitrant

*Laboratoire d'Electromagnétisme, Microondes et Optoélectronique,
Ecole Nationale Supérieure d'Electronique et de Radioélectrique de Grenoble, Boîte Postale 257, 38016 Grenoble CEDEX, France*

M. Haelterman

*Service d'Optique Théorique et Appliquée, Université Libre de Bruxelles, 50 avenue F. D. Roosevelt,
Code Postale 194/5, B-1050 Brussels, Belgium*

(Received 19 June 1990; revised manuscript received 21 June 1991)

We develop a one-dimensional theory of diffraction-induced transverse effects in nonlinear Fabry-Pérot resonators addressed by finite-width incident beams. This is achieved in the framework of the coupled-mode analysis, which takes full advantage of the fact that nonlinear Fabry-Pérot devices are resonant. As compared with a recently published theory dealing with the same subject [M. Haelterman, *Opt. Commun.* **75**, 165 (1990); M. Haelterman, G. Vitrant, and R. Reinisch, *J. Opt. Soc. Am. B* **7**, 1309 (1990); and G. Vitrant, M. Haelterman, and R. Reinisch, *ibid.* **7**, 1319 (1990)], where the nonlinearity is introduced in an approximate way, the formalism developed here takes the nonlinearity associated with the optical Kerr effect rigorously into account. This feature has an important consequence: It leads to a theory that can be generalized to the TM case and also to anisotropic nonlinear media. The theory presented here is valid for any value of the angle of incidence. Under normal (or quasinormal) incidence, two counterpropagating modes, having the same absolute value of the wave-vector component parallel to the plane of the mirrors, are resonantly (or nearly resonantly) excited, whereas under oblique incidence, only one of these modes is excited. This allows us to point out that the feedback leading to optical bistability occurs along the direction of propagation of these resonantly excited counterpropagating modes of the nonlinear optical resonator. This explains why optical bistability disappears under oblique incidence. Although developed in the case of nonlinear Fabry-Pérot resonators, this theory applies to a wide range of nonlinear optical resonators such as nonlinear prism couplers, nonlinear grating couplers, nonlinear interference filters, etc. The theory developed here applies whenever the excited electromagnetic field can be accurately described by a single mode or two counterpropagating modes of the nonlinear device. As an example, numerical results are given in the case of a nonlinear multiple-quantum-well Fabry-Pérot-type structure of $\text{Al}_{1-x}\text{Ga}_x\text{As}/\text{GaAs}$ with $\text{Al}_{1-x}\text{Ga}_x\text{As}/\text{AlAs}$ mirrors.

I. INTRODUCTION

Nonlinear (NL) Fabry-Pérot (FP) resonators appear as promising basic elements for all optical signal processing: optical bistability (OB), optical logic, etc. In order to fulfill the need for massively parallel processors, large bidimensional arrays of micro-NLFP resonators are now developed.¹ The reduction of the size of FP resonators is limited by the diffraction phenomenon which appears to be very important for the design of the NLFP resonator. As a result, the influence of transverse effects arising from diffraction has to be taken into account.

Diffraction in NLFP resonators has given rise to important literature²⁻¹⁴ where a variety of situations regarding the geometry of the NLFP resonator, the type of nonlinearity involved, and the theoretical tools used are reported. Marburger and Felber² treat a high finesse cavity with adjustable focusing elements. Drummond³ considers an interferometer filled with a NL absorber and takes into account the radial variation of the electromagnetic (EM) mode function; dispersive effects and inhomogeneous broadening are also included. Rosanov⁴ discusses the existence of transverse diffusive switching waves. In the paper by Ballagh *et al.*,⁵ the NL medium

is placed in the waist region of a spherical mirror cavity; these authors deal with the "small shaping regime"³ where diffraction can be ignored. As a result, they derive an analytic solution for the cavity transmission and bistability threshold. Firth and Wright⁶ report an analysis of transverse effects in a NLFP resonator with an input Gaussian beam. The method involves projection on to a set of Laguerre-Gaussian functions. Moloney⁷ considers a FP resonator partially filled with a NL medium exhibiting a positive or negative Kerr-type nonlinearity. Firth, Galbraith, and Wright⁸ study the influence of diffusion and diffraction: this is achieved using a quasifast Hankel transformation technique. More recently, Weaire and Kermodé⁹ and Reinisch and Vitrant¹⁰ concentrate on NLFP resonators completely filled, respectively, with self-defocusing and self-focusing media. Olin and Sahlén¹¹ assume a cylindrical symmetry and treat a FP resonator filled with a saturable medium; Olin¹² analyzes the case of dispersive OB in NLFP where diffraction and diffusion are equally strong. The influence of heat conduction, together with the corresponding diffusive process, is considered in Ref. 13. In every case, large differences are found between plane-wave and finite-width-beam calculations.

The papers denoted as Refs. 6–13 have the following common feature: the study of transverse effects is performed without taking into account that, according to the value of the input power involved, the transverse field map (along y , Fig. 1) can be accurately described by its linear expression.¹⁴ As a result, the unknown EM field is looked for as a function of x and y (Fig. 1) leading, in this way, to bidimensional theories. Due to its bidimensional characteristic, this kind of formalism requires large computation times.

Recently, a one-dimensional theory^{15,16} has been developed which relies fully on the fact that NLFP resonators are resonant devices. This theory is based on a pole analysis. As compared to bidimensional theories, the interest of the method of Refs. 15 and 16 is due to simplicity and rapidity because the y dimension has been washed out.

There is however a drawback concerning the pole analysis.^{15,16} In this theory, the linear equation describing the x behavior of the transmitted field is first derived. This equation involves the propagation constant of the linear mode. The nonlinear equation is then obtained by replacing this propagation constant by a nonlinear one which takes into account its dependence on the mode intensity. This is done without any demonstration and the validity is only checked numerically by comparison with the bidimensional calculation. A rigorous demonstration of this treatment is given in the present paper.

We show here that it is possible to develop a one-dimensional theory of diffraction in NLFP resonators illuminated by a finite-width beam under any angle of incidence, where the optical Kerr effect is rigorously accounted for. This is achieved in the framework of the coupled-mode analysis.¹⁷ This formalism is particularly well suited for the study of diffraction in NLFP resonators because the nonlinearity introduces itself naturally from the very beginning of the calculation.

The coupled-mode analysis first requires us to characterize the modes of the linear FP resonator. This is done in Sec. II. Section III is devoted to the determination of the NL equation which describes the coupling between the incident field and the excited modes. A local Kerr nonlinearity is assumed. This equation is compared with

the corresponding one in Ref. 16. The results of Secs. II and III are discussed in Sec. IV where it is shown that, although derived for NLFP resonators, the NL coupling equation also applies to NL prism couplers, NL grating couplers, and NL interference filters. In this section, for the sake of completeness, the main results of Ref. 16, which only concern transverse effects in transmission, are summarized. We then consider a nonlinear multiple-quantum-well Fabry-Pérot-type structure of $\text{Al}_{1-x}\text{Ga}_x\text{As}/\text{GaAs}$ with $\text{Al}_{1-x}\text{Ga}_x\text{As}/\text{AlAs}$ mirrors working in reflection.

II. MODES OF A LINEAR FABRY-PÉROT DEVICE

Let $r_1, t_1; r_2, t_2$ be the linear reflection and transmission coefficients, in amplitude, of, respectively, the front and back mirrors of the FP resonator. It is an easy matter to show that the linear plane-wave transfer function is given by the following expression:

$$\tau(\beta) = \frac{t^2 e^{j\phi_0(\beta)}}{1 - r^2 e^{j2\phi_0(\beta)}} \quad (1)$$

with $t^2 = t_1 t_2$, $r^2 = r_1 r_2$, $\beta = k_0 \sin \theta$, θ the angle of incidence, $k_0 = (\omega/c)n$, n the index of refraction of the outside medium, c the speed of light in vacuum, ω the angular frequency of the incident beam,

$$\phi_0(\beta) = e(k^2 - \beta^2)^{1/2}, \quad (2)$$

e the thickness of the FP resonator, $k = (\omega/c)\sqrt{\epsilon}$, and ϵ the linear relative permittivity of the NL medium, assumed lossless, located between the two mirrors—thus ϵ is real.

Let

$$t^2 = |t|^2 e^{j\psi_t}, \quad r^2 = |r|^2 e^{j\psi_r}.$$

According to Eq. (2), one sees that it is β^2 , and not β , which enters the expression of $\tau(\beta)$. Thus it is more convenient to consider the functions ϕ_0 and τ as functions of β^2 instead of β , i.e., $\phi_0 = \phi_0(\beta^2)$ and $\tau = \tau(\beta^2)$.

Any resonance m of $\tau(\beta^2)$ is associated with a pole $\Gamma_m = \gamma_m^2$ of this function. The pole γ_m^2 fulfills

$$1 - r^2 e^{j2\phi_0(\gamma_m^2)} = 0. \quad (3)$$

In Eqs. (1) and (3) r is a function of β . However in many experimental situations the function $r(\beta)$ is a slowly varying function of β in the resonance domain of interest. Thus we neglect the β dependence of r .

Let

$$\gamma_m^2 = \rho_m^2 + j\kappa_m^2. \quad (4a)$$

Equation (3) yields

$$\rho_m^2 = k^2 - \frac{1}{e^2} [(m\pi - \frac{1}{2}\psi_r)^2 - (\ln|r|)^2], \quad (4b)$$

$$\kappa_m^2 = -\frac{2}{e^2} (m\pi - \frac{1}{2}\psi_r) \ln|r|. \quad (4c)$$

The quantity γ_m^2 is a simple pole of $\tau(\beta^2)$. Since γ_m is complex, γ_m describes leaky modes of the FP resonator.

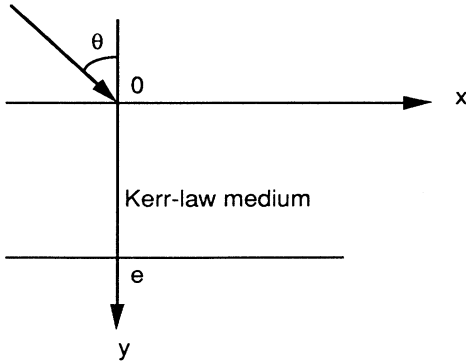


FIG. 1. Geometry considered in this paper.

This leaky feature comes from the fact that $|r| < 1$, i.e., one deals with an open resonator. Assuming a sufficiently high finesse cavity, in the vicinity of a pole Γ_m , the Laurent expansion¹⁸ of $\tau(\beta^2)$ can be approximated by the following expression:

$$\tau(\beta^2) = \tau_m(\beta^2) = \frac{c_m}{\beta^2 - \gamma_m^2} \quad (5)$$

with

$$c_m = \lim_{\beta^2 \rightarrow \gamma_m^2} (\beta^2 - \gamma_m^2) \frac{t^2 e^{j\phi_0(\beta^2)}}{1 - r^2 e^{j2\phi_0(\beta^2)}}.$$

We get

$$c_m = j \frac{t^2}{re^2} (-1)^{m+1} (m\pi + j \ln r). \quad (6a)$$

In the case of high-reflectivity mirrors ($r \approx 1$), the use of Eq. (6a) together with Eq. (4c) yields

$$c_m = j (-1)^{m+1} \frac{e^{j\psi_t}}{1 - (\psi_r/2m\pi)} k_m^2. \quad (6b)$$

Equation (5) provides a suitable basis to discuss which modes are excited when the angle of incidence θ is varied. This equation can be rewritten as

$$\tau_m = \frac{c_m}{k_0^2 \sin^2 \theta - \gamma_m^2}. \quad (7)$$

From Eq. (7), it is seen that one has to distinguish between the two situations θ equal or close to zero and θ different from zero. Let us assume that the wavelength is a fixed parameter.

(i) $\theta = 0$

$$\tau_m = -\frac{c_m}{\gamma_m^2}.$$

Resonance occurs when

$$\text{Re}(\gamma_m^2) = \rho_m^2 = 0. \quad (8a)$$

If we let $\gamma_m = \gamma'_m + j\gamma''_m$, Eq. (8a) shows that

$$|\gamma'_m| = |\gamma''_m|. \quad (8b)$$

Besides this, according to Eq. (4b) Eq. (8a) leads to the value e_m of e for which the leaky mode m is resonantly excited:

$$k^2 e_m^2 = [(m\pi - \frac{1}{2}\psi_r)^2 - (\ln|r|)^2]. \quad (8c)$$

That is to say, under normal incidence, two counterpropagating leaky modes (labeled m) of the FP resonator are resonantly excited provided Eq. (8c) is fulfilled. These two modes have longitudinal x -wave-vector components $\pm |\gamma'_m|$.

(ii) $\theta \neq 0$

$$\tau_m = \frac{c_m}{(k_0 \sin \theta - \gamma_m)(k_0 \sin \theta + \gamma_m)}.$$

Only one leaky mode m is resonantly excited provided:

$k_0 \sin \theta = \pm \text{Re}(\gamma_m)$. This equation can be solved either with respect to e or θ . If the variable of interest is the thickness e , for a given θ this relation leads to the value e_m of e for which resonance occurs:

$$k^2 e_m^2 = \frac{[(m\pi - \frac{1}{2}\psi_r)^2 - (\ln|r|)^2]}{1 - (k_0^2/k^2) \sin^2 \theta}.$$

Due to the nonzero value of θ , it is also possible to derive the value θ_m of θ for which there is resonance (the thickness e being given): $k_0 \sin \theta_m = \pm \text{Re}(\gamma_m)$.

III. NONLINEAR COUPLING EQUATION

We are now in a position to derive the NL coupling equation between the incident field and the leaky modes of the NLFP resonator. This is achieved using the coupled-mode approach.¹⁷ We remind the reader that, as already stated in Sec. I, the NFP resonator is filled with a local Kerr medium.

A. Derivation of the general nonlinear coupling equation

The theoretical developments first require us to define the unperturbed system. The latter is constituted by the linear FP resonator without any illuminating beam. Its normal modes are those discussed in Sec. II. The perturbation arises both from the source polarization due to the incident beam and the nonlinearity of the medium filling the NLFP resonator. We make the usual hypothesis^{19,20} according to which the resulting perturbation can be split into two independent components as follows: One accounts for the coupling process between the incident beam and the NLFP resonator. The corresponding source term is calculated considering the associated linear case. The other component accounts for the NL effect and comes from the existence of the optical Kerr effect inside the NLFP resonator.

It has been shown in Refs. 14 and 16 that the results concerning the response of a NLFP resonator derived from the bidimensional theory^{9,10} are in good agreement with the corresponding ones obtained using the NL coupled-mode formalism.¹⁴⁻¹⁶ Since in the bidimensional theory the excitation process and the induced optical Kerr effect are treated rigorously, this agreement justifies the hypothesis of Refs. 19 and 20 according to which the excitation process can be treated as mentioned above. This conclusion holds whatever the shape of the incident beam may be: plane wave or finite width.

The EM field supported by the unperturbed FP can be expanded¹⁷ on the basis of the modes introduced in Sec. II; the coefficients of this expansion do not depend on x . In the presence of the incident beam, these coefficients become functions of the longitudinal x coordinate.¹⁷ The general expressions of the transverse (in the plane perpendicular to x) electric field $\mathcal{E}_T(x, y)$ and magnetic field $\mathcal{H}_T(x, y)$ are given by the following expressions:

$$\begin{aligned} \mathcal{E}_T(x, y) = & \sum_m c_m^+(x) \mathbf{E}_{Tm}^+(y) e^{j\gamma_m x} \\ & + \sum_m c_m^-(x) \mathbf{E}_{Tm}^-(y) e^{-j\gamma_m x}, \end{aligned} \quad (9a)$$

$$\begin{aligned} \mathcal{H}_T(x, y) = & \sum_m c_m^+(x) \mathbf{H}_{Tm}^+(y) e^{j\gamma_m x} \\ & + \sum_m c_m^-(x) \mathbf{H}_{Tm}^-(y) e^{-j\gamma_m x}. \end{aligned} \quad (9b)$$

The quantities $\mathbf{E}_{Tm}^\pm(y) e^{\pm j\gamma_m x}$ and $\mathbf{H}_{Tm}^\pm(y) e^{\pm j\gamma_m x}$ refer, respectively, to the electric and magnetic fields of the forward (+) and backward (-) propagating modes of the unperturbed structure (an $e^{-j\omega t}$ time dependence is assumed). $\mathbf{E}_{Tm}^\pm(y)$ describe the linear transverse electric mode shape of the forward and backward modes m . We assume $d/dz=0$, thus the mode profile is only a function of y .

It is shown in Ref. 17 that the coefficients $c_m^\pm(x)$ fulfill the following equation:

$$\begin{aligned} N_m^\pm \frac{dc_m^\pm}{dx} = & -j\omega \langle \mathbf{E}_{Tm}^{\pm t}(y) \cdot \mathbf{P}^{\text{NL}}(x, y) \rangle e^{\pm j\gamma_m^t x} \\ & - j\omega \langle \mathbf{E}_{Tm}^{\pm t}(y) \cdot \mathbf{P}^L(x, y) \rangle e^{\pm j\gamma_m^t x}. \end{aligned} \quad (10a)$$

In Eq. (10a) the following statements are true. (i) $\langle \rangle$ stands for an integral in the cross-section plane: $\langle \rangle = \int \dots dy$.

$$(ii) N_m^\pm = \langle \mathbf{u} \cdot (\mathbf{E}_{Tm}^\pm \times \mathbf{H}_{Tm}^{\pm t} - \mathbf{E}_{Tm}^{\pm t} \times \mathbf{H}_{Tm}^\pm) \rangle, \quad (10b)$$

where \mathbf{u} is the unit vector along the x axis. The integral in the cross-section plane is calculated from $y = -\infty$ to $y = +\infty$. The superscript t denotes the adjoint structure deduced from the original one by transposition of the dielectric permittivity and the magnetic permeability matrices.¹⁷ Thus the quantity γ_m^t fulfills¹⁷

$$\gamma_m^t + \gamma_m = 0. \quad (10c)$$

(iii) The first bracket accounts for the existence of the optical Kerr effect of the medium filling the FP resonator which gives rise to the NL polarization $\mathbf{P}^{\text{NL}}(x, y)$. The second one describes the in-coupling of the incident beam, the resulting source polarization being $\mathbf{P}^L(x, y)$.

The terms $\mathbf{P}^{\text{NL}}(x, y)$ and $\mathbf{P}^L(x, y)$ couple all the modes of the structure. Thus Eq. (10a) represents an infinite set of first-order coupled NL differential equations. As pointed out in Ref. 17, this set is exact. It is worth noting that Eq. (10a) is valid for the TE and TM cases and also for anisotropic NL media.

In the remainder of the paper, we consider the situation where (i) only two counterpropagating modes $\pm\gamma_m$ may be resonantly excited and (ii) all the other modes are far enough from these two modes such that the expansion of the transverse EM field takes the following form which accounts both for the normal or non-normal incidence situation:

$$\begin{aligned} \mathcal{E}_T(x, y) = & c_m^+(x) \mathbf{E}_{Tm}^+(y) e^{j\gamma_m x} + c_m^-(x) \mathbf{E}_{Tm}^-(y) e^{-j\gamma_m x}, \\ \mathcal{H}_T(x, y) = & c_m^+(x) \mathbf{H}_{Tm}^+(y) e^{j\gamma_m x} + c_m^-(x) \mathbf{H}_{Tm}^-(y) e^{-j\gamma_m x}. \end{aligned} \quad (11a)$$

Let $a_m^\pm(x) = c_m^\pm(x) e^{\pm j\gamma_m x}$; the use of Eqs. (10a) and (10c) leads to

$$\begin{aligned} N_m^\pm \frac{da_m^\pm}{dx} = & \pm j N_m^\pm \gamma_m a_m^\pm - j\omega \langle \mathbf{E}_{Tm}^{\pm t}(y) \cdot \mathbf{P}^{\text{NL}}(x, y) \rangle \\ & - j\omega \langle \mathbf{E}_{Tm}^{\pm t}(y) \cdot \mathbf{P}^L(x, y) \rangle. \end{aligned} \quad (11b)$$

We pursue the TE case and consider isotropic NL media.²¹ Thus

$$\begin{aligned} \mathcal{E} = & \mathbf{e}_z \mathcal{E} \quad \text{and} \quad \mathbf{E} = \mathbf{e}_z E, \\ \mathbf{P}^L = & \mathbf{e}_z P^L, \quad \mathbf{P}^{\text{NL}} = \mathbf{e}_z P^{\text{NL}}, \end{aligned}$$

and \mathbf{e}_z is a unit vector along the z axis where²¹

$$P^{\text{NL}} = \epsilon_0 \chi^{(3)} |\mathcal{E}|^2 \mathcal{E}, \quad \chi^{(3)} = \chi_{zzzz}. \quad (12)$$

According to Eqs. (11a) and (12), Eq. (11b) yields

$$\begin{aligned} \pm \frac{da_m^\pm}{dx} = & j\gamma_m a_m^\pm + j\omega V_m^{\text{NL}} |a_m^+ + a_m^-|^2 (a_m^+ + a_m^-) \\ & + j\omega V_m^L F_i(x), \end{aligned} \quad (13a)$$

where use has been made of the fact that $N_m^+ = -N_m^- = -N_m$.

$$V_m^{\text{NL}} = \epsilon_0 \frac{\langle \chi^{(3)}(y) E_m^2(y) |E_m(y)|^2 \rangle}{N_m}, \quad (13b)$$

$$V_m^L F_i(x) = \frac{\langle E_m(y) P^L(x, y) \rangle}{N_m}. \quad (13c)$$

$F_i(x)$ accounts for the x dependence of the finite-width incident beam at $y=0$. For example, in the case of an incident Gaussian beam

$$F_i(x) = F_i e^{-(x \cos\theta/w_0)^2} e^{j\beta x}.$$

According to Eq. (10b)

$$N_m = \frac{2\gamma_m}{\omega\mu_0} \langle E_m^2 \rangle. \quad (13d)$$

In Eqs. (13b) and (13c), N_m and the numerator of $V_m^L F_i(x)$ involve integrals which have to be calculated over the whole cross-section plane. According to the leaky feature of the modes, each of these integrals diverges. It will be explained in the following section how this difficulty is solved.

Let $g_m(x)$ denote the x dependence of the total electric field of the mode: $g_m(x) = a_m^+(x) + a_m^-(x)$. From Eq. (13a), we get

$$\frac{d^2 g_m}{dx^2} + \gamma_m^2 g_m + \xi_m^{\text{NL}} |g_m|^2 g_m = \xi_m^L F_i(x) \quad (14a)$$

with

$$\begin{aligned} \xi_m^L = & -2\omega\gamma_m V_m^L, \\ \xi_m^{\text{NL}} = & \frac{\omega^2}{c^2} \frac{\langle \chi^{(3)}(y) E_m^2(y) |E_m(y)|^2 \rangle}{\langle E_m^2(y) \rangle}. \end{aligned}$$

Equation (14a) is important since it constitutes the NL coupling equation between the incident field and the EM field constituted by the forward and backward NL guided modes m . It is worth noting that Eq. (14a) holds even in

the case of multiple-beam excitation.

Once $g_m(x)$ is known, the transmitted field \mathcal{E}_t is given by the following expression:

$$\mathcal{E}_t(x) = g_m(x)E_m(y=e), \quad (14b)$$

whereas the reflected one \mathcal{E}_r is derived from the continuity of the tangential component of the electric field at $y=0$:

$$\mathcal{E}_r(x) = g_m(x)E_m(y=0) - F_i(x). \quad (14c)$$

Equation (14c) can be rewritten as

$$\mathcal{E}_r(x) = q_m \mathcal{E}_t(x) - F_i(x), \quad (14d)$$

where

$$q_m = \frac{E_m(y=0)}{E_m(y=e)}.$$

Equation (14d) provides a useful relation between the reflected, transmitted, and incident fields. It is worth noting that this relation is a linear one between $\mathcal{E}_r(x)$, $\mathcal{E}_t(x)$, and $F_i(x)$. This result is a direct consequence of the assumption underlying the coupled-mode analysis; namely, that the transverse field map (along y) corresponds to the linear one.

Use of the steepest-descent method¹⁸ shows that the far-field pattern, in transmission and reflection, is proportional to the Fourier transform of $\mathcal{E}_t(x)$ and $\mathcal{E}_r(x)$, respectively.

B. Comparison with the results of Ref. 16

In order to compare Eq. (14a) with the corresponding equation of Ref. 16, we consider the case where only one beam is incident on the NLFP resonator. Thus

$$F_i(x) = A_i(x)e^{j\beta x} \quad (15a)$$

and

$$g_m(x) = f_m(x)e^{j\beta x}. \quad (15b)$$

From Eqs. (14a) and (15), it is seen that $f_m(x)$ obeys the following NL coupling equation:

$$\frac{d^2 f_m}{dx^2} + 2j\beta \frac{df_m}{dx} + (\gamma_m^2 - \beta^2)f_m + \zeta_m^{\text{NL}}|f_m|^2 f_m = \zeta_m^L A_i(x). \quad (16a)$$

Equation (16a) shows that the resulting NL longitudinal wave-vector component γ_m^{NL} is complex and depends on the local electric-field intensity $|f_m|^2$ through the following relation:

$$(\gamma_m^{\text{NL}})^2 = \rho_m^2 + \zeta_m^{\text{NL}}|f_m|^2 + j\kappa_m^2. \quad (16b)$$

Therefore

$$\Delta_m = \beta^2 - \rho_m^2$$

corresponds to the initial detuning of the NLFP resonator.

It is interesting to consider the situation $\theta=0$ because

in that case, $\beta=0$ and $\Delta_m = -\rho_m^2$. Thus it is seen that under normal incidence, and for self-focusing media, the two modes involved in the OB process fulfill $\rho_m^2 < 0$. An increase of the excited modes intensity leads to an increase of $(\rho_m^{\text{NL}})^2 = \rho_m^2 + \zeta_m^{\text{NL}}|f_m|^2$. Resonant excitation of these two counterpropagating modes occurs when $(\rho_m^{\text{NL}})^2 = 0$.

Let us now calculate the quantities ζ_m^L and ζ_m^{NL} entering Eq. (16a). This is achieved according to the procedure outlined at the beginning of Sec. III A.

1. Determination of ζ_m^L

It is worth noting that the coefficient ζ_m^L does not depend on the shape of the input beam. Thus ζ_m^L can be determined considering a plane wave instead of a finite-width incident beam. In that case, Eq. (16a) yields

$$(\gamma_m^2 - \beta^2)f_m = \zeta_m^L A_i. \quad (17)$$

Besides this, the transmitted field F_{tm} is given by

$$F_{tm} = f_m E_m(y=e). \quad (18)$$

Equations (17) and (18) lead to

$$\frac{F_{tm}}{A_i} = \frac{\zeta_m^L}{\gamma_m^2 - \beta^2} E_m(y=e). \quad (19)$$

Equation (19) is nothing but the transmittivity τ_m of the FP resonator. Comparison of Eqs. (5) and (19) leads to the desired expression of ζ_m^L :

$$\zeta_m^L = j(-1)^m \frac{e^{j\psi_t}}{1 - (\psi_r/2m\pi)} \frac{\kappa_m^2}{E_m(y=e)}. \quad (20a)$$

2. Determination of ζ_m^{NL}

According to Eq. (16a), the optical Kerr effect exhibited by the medium filling the FP resonator leads to new NL eigenmodes of the interferometer with a longitudinal wave-vector component given by Eq. (16b). Thus the quantity γ_m^{NL} , and as a result ζ_m^{NL} , can be derived looking for the homogeneous solution of the NLFP resonator, i.e., without any input beam. The calculation of ζ_m^{NL} can be performed analytically for a thick ($e \gg \lambda$ in the NL material) FP resonator,²² using Jacobi elliptic functions²³ or a numerical method²⁴ for a thin NLFP resonator. For the sake of simplicity, we consider here a thick FP resonator. In this case, one derives the NL phase shift which is related to the effective NL index variation Δn . Once Δn is known, Eqs. (4) yield

$$\Delta(\gamma_m)^2 = 2\Delta n \left[\frac{\omega}{c} \right]^2 \sqrt{\epsilon},$$

which, together with Eq. (16b), leads to the expression of ζ_m^{NL} . Thus

$$\zeta_m^{\text{NL}} = \frac{3}{2}\chi^{(3)} \left[\frac{\omega}{c} \right]^2 \frac{1 + |r_2|^2}{|t_2|^2} |E_m(y=e)|^2. \quad (20b)$$

From Eqs. (16a), (4a), and (20), we see that the quantity

$F_{im}(x)$ obeys the following equation:

$$\frac{d^2 F_{im}}{dx^2} + 2j\beta \frac{dF_{im}}{dx} + (\rho_m^2 - \beta^2 + \xi_m^{\text{NL}} |F_{im}|^2) F_{im} + j\kappa_m^2 F_{im} = -c_m A_i(x) \quad (21)$$

with

$$\xi_m^{\text{NL}} = \frac{\xi_m^{\text{NL}}}{|E_m(y=e)|^2}.$$

In Ref. 16, for the sake of simplicity r and t have been assumed real. Within the same approximation, Eq. (21) is the same as Eq. (13) of Ref. 16. Such a result justifies *a posteriori* the method used in this reference to include the nonlinearity.

IV. DISCUSSION

The NL coupling equations (14a) and (21) are valid for any incidence: normal, quasinormal, or oblique. As a result, the formalism developed here allows the study of not only NLFP resonators but also NL prism couplers or NL grating couplers. Indeed, as has been already noticed,²⁴ all these devices belong to the class of nonlinear optical (NLO) resonators: the EM resonance involved in NL prism couplers or NL grating couplers is the NL guided mode resonance whereas for NLFP resonators it is the NL Airy resonance.²⁴

When a NLO resonator is excited under oblique incidence, only one mode is involved; the corresponding situation has already been studied by Carter and Chen.¹⁹ It is an easy matter to check that under oblique incidence, Eq. (21) yields Carter and Chen's equation. But for devices which are usually illuminated under normal or quasinormal incidence, two counterpropagating modes are resonantly excited; this fact needs to be included in the theory. Thus the theory developed in this article extends Carter and Chen's analysis to the case of NLO resonators illuminated under small incidence angles with respect to the resonance width in the θ domain.

2. Transverse effects in transmission

Extensive numerical results concerning the behavior of the response of NLFP resonators when varying the finesse, the width w_0 of the incident beam, and the angle of incidence can be found in Ref. 16 where the emphasis was only on the transmitted beam. We first summarize the main results obtained there (Ref. 16) and then consider a nonlinear device working in reflection. In Ref. 16 the following has been shown.

(a) For normal incidence and for self-focusing media there is an OB loop even for tightly focused beams. This is a consequence of the existence of a self-focusing channel of light in the NLFP resonator. For self-defocusing media, the OB loop disappears when w_0 decreases.

(b) Under oblique incidence two facts are shown. (i) There exists a limiting value θ_l of θ beyond which ($\theta > \theta_l$) OB is lost. This conclusion may be understood on the basis of Secs. II and III. Under normal incidence, the optical Kerr effect allows a simultaneous retuning of the

forward and backward propagating modes m . On the other hand, under oblique incidence only one mode may be resonantly excited (forward or backward, depending on the sign of θ). Therefore it is seen that the feedback giving rise to OB occurs along the x direction since it comes from the resonant excitation of two counterpropagating modes. In the case of oblique incidence, feedback is lost and OB disappears. Consequently the zig-zag path inside the NL resonator does not introduce the necessary feedback to get OB, it only allows for the existence of NL eigenmodes of the structure. (ii) Concerning the variation of θ_l with the width w_0 of the input beam, it has been found¹⁶ that an increase of w_0 leads to a decrease of θ_l : the larger the input beam, the smaller the θ range yielding OB. This result is surprising because when considering an incident plane wave, OB exists whatever the value of θ may be. The reason for this behavior of θ_l comes from the fact that the Fourier spectrum of the incident beam in the wave vector domain, which is linked to the diffraction effect, is all the more important than w_0 is small. Everything happens as if the finite-width incident beam was behaving as a wave-vector generator. It is this wave-vector generator which allows the simultaneous resonant excitation of the two counterpropagating modes even when θ is different from zero. Since this generator includes fewer and fewer wave vectors as w_0 increases, one understands why θ_l decreases when w_0 increases. In addition, it is seen that under non-normal incidence, the plane-wave solution is never recovered both for self-focusing and self-defocusing media. This is also the case for normal incidence, but only for positive Kerr media.¹⁶

To summarize, it has been shown that considering a local Kerr medium, there is no OB under oblique incidence in the case of a finite-width incident beam. This result contradicts the conclusion of Refs. 24–26, dealing with plane-wave excitation, where it is shown that OB occurs even under oblique incidence. As explained in Ref. 14, the existence of OB under oblique incidence with plane waves is due to the fact that a plane-wave calculation introduces an “artificial” feedback through the implicit assumption that the NL index of refraction is independent from x . In fact, plane-wave calculations describe experimental situations where a completely delocalized nonlinearity²⁷ is involved. In this paper, we concentrate on a local nonlinearity. Moreover, the result of Ref. 28—according to which there should be OB under oblique incidence, even in the case of a finite-width incident beam—has been shown²⁹ to arise from the approximation made in Ref. 28, where it is assumed that the NL index of refraction has no x dependence. Again this hypothesis introduces an “artificial” feedback which explains the existence of OB reported in Ref. 28.

B. Transverse effects in reflection

For the sake of specificity, let us now consider the case of a nonlinear multiple-quantum-well Fabry-Pérot-type structure of $\text{Al}_{1-x}\text{Ga}_x\text{As}/\text{GaAs}$ with $\text{Al}_{1-x}\text{Ga}_x\text{As}/\text{AlAs}$ mirrors (Fig. 2). Such a device works in reflection

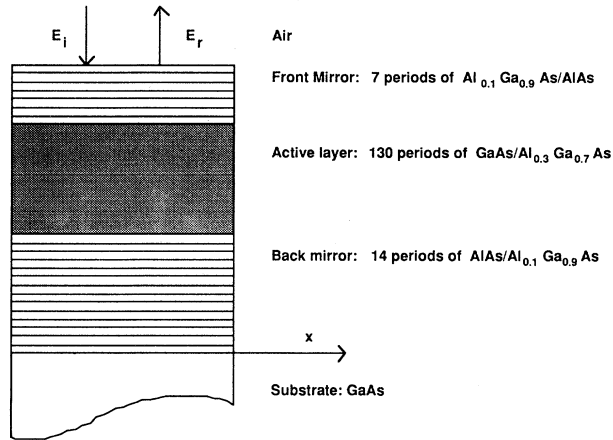


FIG. 2. Geometry of the nonlinear multiple-quantum-well Fabry-Pérot-type structure of $\text{Al}_{1-x}\text{Ga}_x\text{As}/\text{GaAs}$ with $\text{Al}_{1-x}\text{Ga}_x\text{As}/\text{AlAs}$ mirrors.

and corresponds to a recently published structure.³⁰

The front and back mirrors are assumed linear and are constituted by, respectively, 7 and 14 periods of quarter-wave layers of $\text{AlAs}/\text{Al}_{0.1}\text{Ga}_{0.9}\text{As}$ such that their reflectivities in intensity are $R_F=91.7\%$ and $R_B=97.6\%$. The refractive indices of AlAs , GaAs , and $\text{Al}_{0.1}\text{Ga}_{0.9}\text{As}$ are, respectively, chosen equal to 2.956, 3.660, and 3.551 at a wavelength in vacuum of 840 nm. The active medium exhibits a negative Kerr effect and consists of 130 periods of alternating (~ 10 nm) GaAs and $\text{Al}_{0.3}\text{Ga}_{0.7}\text{As}$ layers. We have checked that it is possible to replace it by a single layer with an averaged complex refractive index n_0 equal to $3.537 + j6.7 \times 10^{-4}$.

The layers of the mirrors are quarter-wave ones at a wavelength $\lambda=838$ nm, and the thickness of the central layer is chosen equal to $2.7258 \mu\text{m}$. In order to determine the reflected field of the NL device (Fig. 2), it is convenient to consider first the associated linear device.

(a) *Associated linear device.* In the plane-wave case, there exists a linear relation between the reflected field $\mathcal{F}_{rm,lin}(\beta)$, the transmitted one $\mathcal{F}_{tm,lin}(\beta)$, and the amplitude $\mathcal{A}_i(\beta)$ of the incident plane wave which may be written as

$$\mathcal{F}_{rm,lin}(\beta) = p_m \mathcal{A}_i(\beta) + q_m \mathcal{F}_{tm,lin}(\beta), \quad (22)$$

where $\mathcal{F}_{tm,lin}(\beta)$ is simply derived using Eq. (21) and p_m and q_m are two constant complex coefficients nearly independent of β in the vicinity of the resonance m . Thus in the case of a finite-beam-width excitation, the reflected field spatial distribution $F_{rm,lin}(x)$ is related to the transmitted one $F_{tm,lin}(x)$, by the following relation:

$$F_{rm,lin}(x) = p_m A_i(x) + q_m F_{tm,lin}(x). \quad (23)$$

(b) *NL device.* The following is worth noting. According to their definitions, p_m and q_m only depend on the features of the linear transverse field map. Therefore, in the framework of the coupled-mode analysis used in this

TABLE I. Numerical values of the parameters for the modal theory.

Parameter	Value
γ_m^2	$1.8901 \times 10^{12} + j0.61878 \times 10^{12} \text{ m}^{-2}$
c_m	$-j0.1805 \times 10^{12} \text{ m}^{-2}$
ξ_m^{NL}	$-3.701 \times 10^{15} \text{ V}^{-2}$
p_m	$-0.9927 + j0.00055$
q_m	$3.586 + j0.0157$

paper, these quantities keep the same expression in the NL case. In addition, Eq. (22) remains a linear equation between the reflected, the transmitted, and the incident fields. Thus considering now the NL device (Fig. 2), we get

$$F_{rm}(x) = p_m A_i(x) + q_m F_{tm}(x), \quad (24)$$

where $F_{tm}(x)$ is given by the full NL Eq. (21) and $F_{rm}(x)$ is the reflected field map. Equation (24) is a generalization of Eq. (14d) to the case of a multilayered NL structure. Thus for a NLFP resonator the coefficient p_m is equal to -1 . In the case of the NL device (Fig. 2), the values of the coefficients ρ_m^2 , κ_m^2 , c_m , ξ_m^{NL} , q_m , and p_m have been derived by a fit considering the plane-wave excitation of the NL device (Fig. 2). The corresponding exact reflectivity has been determined extending the method of Ref. 24 to the case of a multilayered nonlinear structure.

The numerical values of the parameters obtained for this structure are given in Table I. For the NL device (Fig. 2), the resonance under normal incidence occurs at $\lambda=838.3$ nm. Thus the threshold for bistability is at 837.62 nm and we consider a working wavelength at 837.12 nm for which bistability exists with plane waves.

It is seen in Fig. 3 that the agreement between the modal reflectivity obtained from Eq. (24) and the exact reflectivity is excellent. Hence, we use these tested coefficients to study the transverse effects in the nonlinear structure (Fig. 2) illuminated by an incident Gaussian beam.

The influence of the incident beam width w (w is full width at half intensity) on the response of the nonlinear FP resonator is analyzed at normal incidence. Figure 4

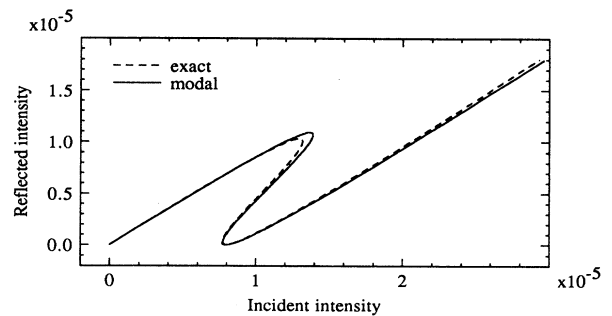


FIG. 3. Comparison between the exact and modal theories in the plane-wave case. Normal incidence.

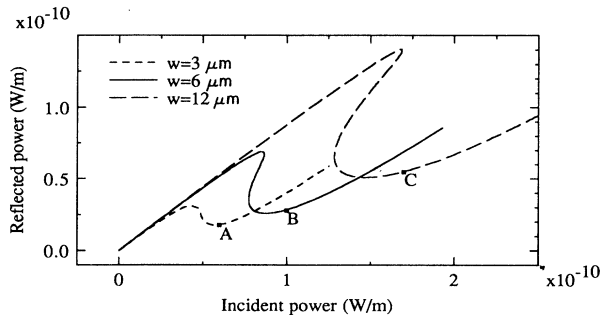


FIG. 4. Response of the device for three incident beam widths w (w is full width at half intensity).

shows the bistability curves in reflection for Gaussian beams whose waists are $w = 3, 6,$ and $12 \mu\text{m}$. The total reflected power integrated across the beam section is plotted versus the total incident power. It is seen that for a given detuning there exists a minimum waist for bistability.

We are now interested in the beam profiles after the commutation occurs, when the nonlinear term is high, here for the working points $A - C$ of Fig. 4 corresponding to the three waists. Due to self-defocusing, the transmitted (not observable experimentally) profile (Fig. 5) shows a smooth shape, contrary to the self-focusing case.^{10,14,16} In fact the transmitted beam is spatially narrower (after the commutation) than the incident one, since the commutation only occurs at the center where the incident intensity is high enough. This leads to the existence of sidebands in the reflected beam. In addition, the saturation of the nonlinear transmittivity, together with the self-defocusing spatial spread out of the transmitted beam, explains the existence of a peak at the center of the reflected beam. This qualitatively explains the typical shape which is constituted of a central peak with sidebands in the reflected far-field pattern (Fig. 6).

V. CONCLUSION

It has been shown in this paper that the coupled-mode formalism is particularly well suited for the study of

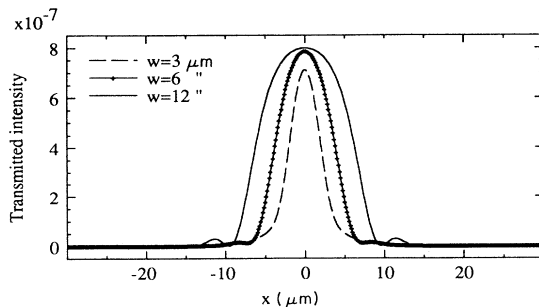


FIG. 5. Transmitted profiles for working points $A - C$ of Fig. 4: near field at the substrate interface (w is full width at half intensity).

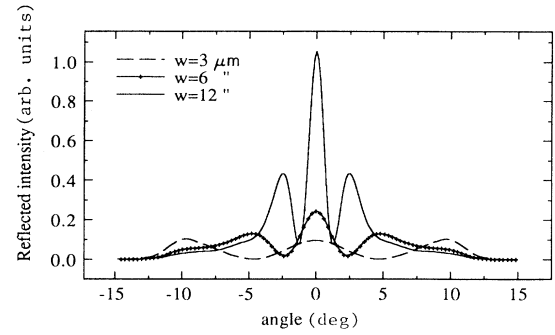


FIG. 6. Reflected profiles for working points $A - C$ of Fig. 4: far field at infinity (w is full width at half intensity).

transverse effects in NLO resonators. It is worth noting that this is achieved by rigorously taking into account the optical Kerr effect. Moreover, this formalism also allows us to study the transverse effects in the NLO resonator including anisotropic Kerr-law media whatever the polarization of the incident beam(s) (TE or TM) may be. As compared with bidimensional analysis,⁶⁻¹³ the theory developed here takes full advantage of the resonant feature of the NL device. One may think that this resonant requirement corresponds to a limitation. This is not the case because¹⁶ the NL coupling equation applies to NLO resonators whose finesse is as low as 5. In addition, the theory presented here leads to a strong reduction¹⁶ in the computation time as compared to bidimensional analysis: of the order of 100. This allows a systematic study of diffraction effects in NLO resonators, for example, the influence of $\theta, w_0,$ the finesse, etc. on the optical response of the NL device in transmission as well as in reflection. As already mentioned, this theory applies not only to NLFP resonators but also to NL prism couplers and NL grating couplers. In fact, this analysis applies whenever it is possible to isolate a single EM resonance (in the β^2 domain), i.e., each time the associated linear transmittivity can be approximated by a Lorentzian in the vicinity of the nearest EM resonance. This extends the range of application of the NL coupling equation to NL prism couplers, NL grating couplers, and NL interference filters^{31,32} but excludes superlattices^{32,33} because in this case the spacing between the EM resonances is nearly equal to their width. The features of the NL device enter Eq. (14a) through ξ_m^L and ξ_m^{NL} . In the case of NLFP and NL prism couplers, an analytical calculation, using the method of Sec. III, is possible. When dealing with the NL grating couplers or NL interference filters, a fitting method based on the numerical plane-wave calculation has to be used.

Since the NL coupled-mode theory presented here applies to bulk devices (such as NLFP or NL interference filters) and also to devices in the guided-wave geometry (such as NL prism couplers or NL grating couplers), it is not the bulk or guided-wave characteristic of the geometry of these devices which is important. The important feature is the ability of these NL devices to exhibit an EM resonance (NL Airy resonance for NLFP reso-

nators, NL guided-mode resonance for NL prism couplers or NL grating couplers). It is this feature which leads to the possibility of using a coupled-mode theory, usually developed for guided-wave devices, even for bulk NL resonators. Thanks to the "guided-wave" type of the theory, we have shown that the feedback leading to OB takes place along the x direction. This explains why no OB is obtained under oblique incidence.^{19,16} This study is only concerned with local Kerr media. But the formalism we have developed can be generalized to include non-local effects. This has already been done for NL prism couplers.²⁷

According to its wide range of applications, it is seen that this coupled-mode analysis of transverse effects provides a powerful tool for the study and design of micro-NLO resonators where diffraction-induced transverse effects cannot be neglected.

ACKNOWLEDGMENTS

R.R. and G.V. would like to acknowledge support from DRET Contract No. 89-189. The work of M.H. was partly supported by the FNRS and the IAP program of the Belgium government.

-
- ¹J. L. Jewell, A. Scherer, S. L. McCall, A. C. Gossard, and J. H. English, *Appl. Phys. Lett.* **51**, 94 (1987).
²J. H. Marburger and F. S. Felber, *Phys. Rev. A* **17**, 335 (1978).
³P. D. Drummond, *IEEE J. Quantum Electron.* **QE-17**, 301 (1981).
⁴N. N. Rozanov, *Zh. Eksp. Teor. Fiz.* **80**, 96 (1981) [*Sov. Phys.—JETP* **53**, 47 (1981)].
⁵R. J. Ballagh, J. Cooper, M. W. Hamilton, W. J. Sandle, and D. M. Warrington, *Opt. Commun.* **37**, 143 (1981).
⁶W. J. Firth and E. M. Wright, *Opt. Commun.* **40**, 233 (1982).
⁷J. V. Maloney, *Opt. Acta.* **29**, 1503 (1982).
⁸W. J. Firth, I. Galbraith, and E. M. Wright, *J. Opt. Soc. Am. B* **2**, 1005 (1985).
⁹D. Weaire and J. P. Kermodé, *J. Opt. Soc. Am. B* **3**, 1706 (1986).
¹⁰R. Reinisch and G. Vitrant, *J. Appl. Phys.* **67**, 6671 (1990).
¹¹U. Olin and O. Sahlén, *J. Opt. Soc. Am. B* **4**, 319 (1987).
¹²U. Olin, *J. Opt. Soc. Am. B* **5**, 20 (1988).
¹³U. Olin, *J. Opt. Soc. Am. B* **7**, 35 (1990).
¹⁴G. Vitrant, *Thèse d'état*, Institut National Polytechnique de Grenoble, 1989.
¹⁵M. Haelterman, *Opt. Commun.* **75**, 165 (1990). M. Haelterman, G. Vitrant, and R. Reinisch, *J. Opt. Soc. Am. B* **7**, 1309 (1990).
¹⁶G. Vitrant, M. Haelterman, and R. Reinisch, *J. Opt. Soc. Am. B* **7**, 1319 (1990).
¹⁷H. Kogelnik, in *Integrated Optics*, edited by T. Tamir, Topics in Applied Physics Vol. 7 (Springer-Verlag, New York, 1975), Chap. 2; C. Vassalo, *Théorie des Guides d'Ondes Electromagnétiques* (Eyrolles, Paris, 1985), Vols. 1 and 2. The adjoint structure is introduced in this reference; J. E. Sipe and G. I. Stegeman, *J. Opt. Soc. Am.* **69**, 1676 (1979).
¹⁸G. Arfken, in *Mathematical Methods for Physicists* (Academic, New York, 1970).
¹⁹G. M. Carter and Y. J. Chen, *Appl. Phys. Lett.* **42**, 643 (1983).
²⁰C. Liao and G. I. Stegeman, *Appl. Phys. Lett.* **44**, 164 (1984).
²¹J. W. Nibler and G. V. Knighten, in *Raman Spectroscopy of Gases and Liquids*, edited by A. Weber (Springer-Verlag, New York, 1979), p. 243.
²²F. S. Felber and J. H. Marburger, *Appl. Phys. Lett.* **28**, 731 (1976).
²³W. Chen and D. L. Mills, *Phys. Rev. B* **35**, 524 (1987).
²⁴R. Reinisch and G. Vitrant, *Phys. Rev. B* **39**, 5775 (1989).
²⁵B. Bosacchi and L. M. Narducci, *Opt. Lett.* **8**, 324 (1983).
²⁶V. J. Montemayor and R. T. Deck, *J. Opt. Soc. Am. B* **2**, 1010 (1985).
²⁷G. Vitrant, R. Reinisch, J. Cl. Paumier, G. Assanto, and G. I. Stegeman, *Opt. Lett.* **14**, 898 (1989).
²⁸V. J. Montemayor and R. T. Deck, *J. Opt. Soc. Am. B* **3**, 1211 (1986).
²⁹G. Vitrant, P. Arlot, and R. Reinisch, *Proc. SPIE* **800**, 169 (1987).
³⁰B. Sfez, J. L. Oudar, J. C. Michel, R. Kuszelewicz, and R. Azoulay, *Appl. Phys. Lett.* **57**, 324 (1990); J. L. Oudar, B. Sfez, R. Kuszelewicz, J. C. Michel, and R. Azoulay, *Phys. Stat. Solidi* (to be published).
³¹F. V. Karpushko and G. V. Sinityn, *J. Appl. Spectrosc. (USSR) Proc.* **29**, 1323 (1978); B. S. Wherrett, D. Hutchings, and D. Russel, *J. Opt. Soc. Am. B* **3**, 351 (1986).
³²J. Danckaert, K. Fobelets, G. Cauwenberghs, and I. Veretenicoff, *Proc. SPIE*, 1280 (1990).
³³W. Chen and D. L. Mills, *Phys. Rev. B* **36**, 6269 (1987).